Vrije Universiteit Brussel

In-situ odd random phase electrochemical impedance spectroscopy study on the electropolymerization of pyrrole on iron in the presence of sodium salicylate - The influence of the monomer concentration

Cysewska, Karolina; Macia, Lucia Fernandez; Jasinski, Piotr; Hubin, Annick

Published in:
Electrochimica Acta

DOI:
10.1016/j.electacta.2018.09.069

Publication date:
2018

License:
CC BY-NC-ND

Document Version:
Accepted author manuscript

Link to publication

Citation for published version (APA):
Cysewska, K., Macia, L. F., Jasinski, P., & Hubin, A. (2018). In-situ odd random phase electrochemical impedance spectroscopy study on the electropolymerization of pyrrole on iron in the presence of sodium salicylate - The influence of the monomer concentration. *Electrochimica Acta*, *290*, 520-532. https://doi.org/10.1016/j.electacta.2018.09.069

Copyright
No part of this publication may be reproduced or transmitted in any form, without the prior written permission of the author(s) or other rights holders to whom publication rights have been transferred, unless permitted by a license attached to the publication (a Creative Commons license or other), or unless exceptions to copyright law apply.

Take down policy
If you believe that this document infringes your copyright or other rights, please contact openaccess@vub.be, with details of the nature of the infringement. We will investigate the claim and if justified, we will take the appropriate steps.

Download date: 10. Apr. 2024

In-situ odd random phase electrochemical impedance spectroscopy study on the electropolymerization of pyrrole on iron in the presence of sodium salicylate – the influence of monomer concentration

Karolina Cysewska [1,2,*], *Lucía Fernández Macía* [2], *Piotr Jasiński* [1], *Annick Hubin* [2]

[1] Faculty of Electronics, Telecommunications and Informatics, Gdansk University of Technology, ul. Narutowicza 11/12, 80-233 Gdansk, Poland

[2] Research group Electrochemical and Surface Engineering, Vrije Universiteit Brussel, Pleinlaan 2, 1050 Brussels, Belgium

*E-mail: Karolina.Cysewska@vub.be, kar.cysewska@gmail.com

ABSTRACT

In this work, potentiostatic electropolymerization of polypyrrole (PPy) on iron in aqueous solution of sodium salicylate and pyrrole is studied in-situ by odd random phase electrochemical impedance spectroscopy (ORP-EIS). The influence of the pyrrole concentration on the electrosynthesis process is investigated. The ORP-EIS technique ensures reliable analysis of PPy electrosynthesis on iron based on the advanced data analysis of the level of non-linear and/or non-stationary behaviour and the signal-to-noise ratio of the system. Additionally, the PPy/Fe material is analysed with scanning electron microscopy (SEM), energy dispersive X-ray spectroscopy (EDX) and glow discharge optical emission spectroscopy (GDOES). The surface analysis techniques confirm the presence of the passivation layer at the PPy/iron interface formed prior to the polymer deposition. The modelling of the EIS over time provides the quantitative analysis of the electropolymerization of PPy on iron. The results show that the electrosynthesis process of pyrrole on oxidizable iron in the presence of sodium salicylate is a complex process, which includes not only

reactions of pyrrole oxidation but also reactions such as the oxidation/reduction of the iron surface and/or reactions between the iron, formed interlayer and polypyrrole.

Keywords: in-situ odd random phase electrochemical impedance spectroscopy, polypyrrole, iron, sodium salicylate, electropolymerization

1. Introduction

Current cardiovascular stent technology is mostly based on the use of permanent stents made from corrosion-resistant metals [1,2]. These are mainly stainless steel 316L, but tantalum, nitinol, cobalt alloy and platinum iridium are commercially used as well [3]. Recent studies have shown that the presence of such a material for long time in the human body can cause re-overgrowing of the tissue within the treated portion of the vessel, which leads to the re-blockage of the circulatory system and many other clinical complications [2,3]. Thus, research on biodegradable metallic stents is conducted at present [1–3]. The materials for this purpose are active/oxidizable metals and their degradation is based on their progressive corrosion. One interesting metal for this application is iron [3,4]. However, in order to use iron in clinical applications, its degradation rate and biological performance need to be optimized [3–5]. A favourable solution is to modify the metallic surface with conducting polymer films [6–9].

Recently, research on conducting polymers has become very important in different technological areas [10–12]. The major property of these polymers is their metallic-like conductivity resulting from the conjugated double bond in their backbone [10]. Polypyrrole (PPy) is one of the promising conducting polymers that exhibits very good environmental stability [11], excellent mechanical and thermal properties [11] and high biocompatibility [13]. Due to its unique properties, polypyrrole has been used as advanced coating material in many applications such as anti-corrosive coatings [9,14,15], biosensors [16,17] organic electronics [18] or biomaterials [9,19].

It is well known that conducting polymer films can be synthesized chemically or by electrochemical route [10]. The latter option is more favourable due to its simplicity, low cost and high reproducibility [20]. Besides, it allows controlling different properties of the polymeric material [21]. The electropolymerization process leads to the formation of a positively charged polymer with counter-anions incorporated into its structure [22].

Both the properties of the polymeric layer and the mechanism of its synthesis are directly influenced by the experimental conditions of the electropolymerization. Thus, the choice of parameters, such as type of electrolyte/solvent, applied current density or potential, will strongly affect the synthesis process [21,23,24]. Another important element that influences the electropolymerization process is the type of substrate [25,26]. It has been noticed that the morphology, structure, conductivity and other physicochemical properties of the polymer films differ depending on the substrate [26]. The electrodeposition of conducting polymers proceeds easily on inert substrates such as platinum, gold or glassy carbon [27,28]. However, the synthesis of these polymers on oxidizable metals is a complex process, which involves different stages of the synthesis. The choice of the wrong synthesis parameters leads to a high dissolution of the metal, which hinders the polymer deposition. This is related to the fact that the oxidation potential of an active metal is much lower than the oxidation potential of the monomer [9]. One way to solve this problem is the proper selection of the type of anions in the supporting electrolyte, which can promote the passivation of the metal surface when it comes in contact with the electrolyte. This inhibits the metal dissolution and allows for a stable polymer deposition [26]. Thus, the electrodeposition of conducting polymers on oxidizable metals is a more challenging and complicated process than on inert substrates.

Polypyrrole has already been electrochemically polymerized on different kinds of active metals such as steel/iron [8,29,30], magnesium [31,32], nickel [27], zinc [28] or copper [33,34] and in presence of several kinds of supporting electrolytes [8,27,30,31]. It has been

observed that the mechanism and the way of the polymer synthesis is directly dependent on the types of active metal and supporting electrolyte [26]. In literature, many studies reveal the passivating properties of oxalate anions during the electropolymerization of pyrrole on iron [35–37] or steel [38]. It has been shown that in the presence of these anions the passivation of iron/steel occurs immediately after the electrosynthesis current or potential is applied. The next stages of the electropolymerization in presence of oxalates are the decomposition of the passivated layer and the subsequent electropolymerization of pyrrole directly on the metallic surface [37,38]. A different behaviour has been seen in the case of salicylate anions for iron [8,9,39], copper [34], magnesium [32] or zinc [28]. Here, the polymer is deposited directly on the passivation layer, which is formed at the beginning of the electropolymerization process. This layer inhibits the metal dissolution and allows for a stable polymer deposition. The composition of the passivation layer is still strongly under debate. Mostly, it is described as a metal oxide/hydroxide and/or a metallic salt. Srinivasan et al. [32] determine the interlayer between magnesium and PPy as a magnesium-salicylate complex. However, El Jaouhari et al. [39] characterize the passivation layer on iron as an iron oxide and/or iron salicylate complex. Similar passivating properties have also been observed in the case of malic acid with iron [40], sulfuric acid with steel [41] or dodecylbenzenesulfonic acid with copper [33]. On the contrary, the electropolymerization of pyrrole on oxidizable metals has not been possible in the presence of poly-styrenesulfonate (PSS) [35,36] or dodecyl sulfate (DS^-) anions [36]. Therefore, the fact that the metal passivation occurs without hindering the polymer deposition demands a careful choice of media and parameters for a successful electropolymerization of pyrrole on active metals. This particularity of the electrosynthesis process makes the direct electrodeposition of PPy possible without any chemical or electrochemical pretreatment.

Previous studies showed that PPy doped with salicylate can increase the corrosion resistance of iron. The level of the protection depends on the synthesis conditions used during

the electropolymerization [8,14]. Polypyrrole film electrosynthesized in the presence of sodium salicylate under different conditions reveals different morphological, electrical and redox properties [8,42,43]. Our previous study has shown that the degradation of iron can be tailored by changing the properties of an electropolymerized salicylate-doped polypyrrole film [9]. Exposed to a human body-like electrolyte, PPy coatings synthesized under certain conditions inhibit the corrosion of iron at the beginning of the immersion and later they enhance the degradation of the material in a steady manner. This characteristic is very desirable in the case of medical applications, such as biodegradable metallic cardiovascular stents. It is also noticed that the passivation interlayer formed on iron surface prior to the PPy electrodeposition has a major impact on the corrosion properties of the coated iron [9]. Therefore, a more detailed study of the synthesis of the polymer doped salicylate film on iron is crucial to gain insight into the processes occurring during the material degradation.

Different measurement techniques have been used to study the electrochemical polymerization of pyrrole on oxidizable metals. Most investigations have been carried out by potential sweep methods [32,34,39,44,45] or under potentiostatic/galvanostatic control [34,35,40,41,46]. Other measurement techniques such as X-ray photoelectron spectroscopy (XPS) [33,41], time-of-flight secondary ions mass spectrometry (ToF-SIMS) [33], electrochemical quartz crystal microbalance (EQCM) [28] or in-situ Raman spectroscopy [37] have also been used to get insight into the polymer electrosynthesis. Moreover, there have been some attempts to study the electropolymerization by electrochemical impedance spectroscopy (EIS) [47,48]. Popkirov et. al [47] study the galvanostatic electrosynthesis of bithiophene on platinum substrate in an acetonitrile solution containing NBt_4BF_4. Based on the EIS measurements it is suggested that three processes occur in the system: charge transfer of the polymerization reaction, charge transfer of the oxidation/reduction reactions of polybithiophene and diffusion of the ions through the polymer film. All are dependent on the

thickness of the polymeric layer [47]. The initial stages of the potentiostatic electropolymerization process of polyaniline (PANI) on platinum from acid aqueous solution are also studied by EIS [48]. For this case, two processes are observed: the charge transfer of the polymerization at high frequencies and a diffusion contribution in the low frequency range, which is associated with the transport of the monomer from the bulk of the electrolyte [48].

In this work, the electrochemical polymerization of pyrrole on iron in an aqueous solution of sodium salicylate is studied in-situ by odd random phase electrochemical impedance spectroscopy (ORP-EIS). Here, ORP-EIS measurements are performed simultaneously with the polymerization process. The impedance spectra are analysed for the electropolymerization of pyrrole on iron. The ORP-EIS technique ensures reliable experimental data and impedance modelling based on the advanced data analysis of the level of non-linear and/or non-stationary behaviour and the signal-to-noise ratio of the system [9,49,50]. Once the quality of the experiments is confirmed, the ORP-EIS data are fitted to the proposed electrical equivalent circuit that represents the electrochemical processes occurring during the electropolymerization. The parameters that describe the electrochemical system are estimated using a statistically founded methodology. The evolution of the parameters describing the polymerization process is analysed. This approach provides a reliable and quantitative study of the PPy electrodeposition on iron in the presence of sodium salicylate. To the best of our knowledge, this subject has not been investigated with this approach before.

2. Experimental

2.1 Chemicals and materials

The chemicals used in this work are: pyrrole monomer (≥ 99%, Acros Organics), sodium salicylate (≥ 99.5%, EMSURE). The solutions are prepared with Mili-Q water. The

substrate is a pure iron plate (≥ 99.8%, Chempur Feinchemikalien und Forschungsbedarf GmbH).

The iron plate is embedded in epoxy resin. Before each polymerization process, the iron electrode is mechanically grinded with abrasive papers 220, 500 and 1200 SiC grade (Struers), rinsed with ethanol and dried.

2.2 Electropolymerization of pyrrole

Besides the EIS study, chronoamperograms of the electropolymerization are performed. The polypyrrole film is potentiostatically synthesized in a one step process at 1.2 V vs. $Ag/AgCl_{sat}$ in aqueous solution of 0.1 M sodium salicylate and 0.05, 0.1 or 0.15 M pyrrole for 1800 s at room temperature. The chosen polymerization potential, sodium salicylate and pyrrole concentration are the conditions that provide the optimum corrosion protection of polypyrrole coating on iron, as demonstrated in our earlier study [9]. The investigation of the synthesis process is presented for three main pyrrole concentrations, which are also the most often chosen in the literature [6,8,15,33,35]. The synthesis process with intermediate pyrrole concentrations does not reveal clear representation of the processes present during the electrodeposition of pyrrole on active iron.

2.3 ORP-EIS study during pyrrole electropolymerization

An odd random phase multisine is used as excitation signal in the ORP-EIS technique. The signal consists of the sum of harmonically related sine waves with randomly generated phases. Only odd harmonics are excited and, per group of 3 consecutive harmonics, one is randomly omitted [49,50]. The multisine signal allows for the reduction of the measurement time. Besides, the non-stationarities and non-linearities of the studied system can be determined. Every ORP-EIS measurement and its noise distortions are obtained from the calculations of 4 multisine periods. The detailed explanation of the technique can be found in previous works [50,51].

The ORP-EIS impedance measurements are performed simultaneously with the electrochemical polymerization of pyrrole on iron at 1.2 V vs. $Ag/AgCl_{sat}$ for 1800 s. The measurements are acquired in a one-compartment, three-electrode cell. The working electrode is the iron plate with an exposed area of 0.38 cm^2. An $Ag/AgCl_{sat}$ is used as reference electrode and a platinum grid, as counter electrode. All current densities in this work are calculated with regard to the exposed area.

The measuring setup consists of a Wenking potentiostat POS 2 (Bank Elektronik) and a National Instrument PCI-4461 DAQ-card with a built-in anti-aliasing filter. The applied multisine signal is digitally composed with MATLAB R2010a software (MathWorks Inc.) MATLAB is also used for processing the collected data and controlling the DAQ-card. The perturbation signal applied is a 3 mV RMS variation around the open circuit potential. The impedance spectrum is acquired in the frequency range of 15 Hz – 50 kHz. The selected frequency range allows observing all important phenomena during electropolymerization and allows for recording EIS with high time resolution, which is particularly important at the beginning of the synthesis process.

2.4 Analysis and fitting of ORP-EIS data

The ORP-EIS technique provides information about the noise level, non-stationary behaviour and non-linear behaviour of the system. Therefore, the analysis enables to assess whether the impedance data have a good signal-to-noise ratio and fulfil the conditions of stationarity and linearity, necessary for correct experimental impedance data [52].

The experimental data are modelled with equivalent electrical circuits (EEC). The quality of the fitting is assessed based on the complex modelling residuals, which is the difference between the model and the experiment. The validation of the EEC modelling is based on the following criteria: (1) the model is physically plausible; (2) the modelling

residual is low with regard to the noise level; (3) the estimated parameters are physically explicable and have a low standard deviation.

2.5 Surface analysis

The cross-sectional images, energy dispersive X-ray (EDX) analysis and elemental mapping of PPy/Fe electrode are acquired using a field emission scanning electron microscope (FE-SEM) JEOL JSM-7100F with a lateral resolution of 1.2 nm at 30 kV, 3 nm at 1 kV and 3.0 nm at 15 kV, with a working distance of 10 mm and a probe current of 5 nA. The instrument is also equipped with a through-the-lens (TTL) system, which provides high resolution at very low landing electron energy (100 eV). It is coupled with an Oxford Instruments WAVE WDX spectrometer, with four analysing crystals and an integrated SDD X-Max 20 mm^2 EDX detector. The energy resolution ranges from 127 eV for the EDX to 10 eV for the WDX system. Glow discharge optical emission spectroscopy (GDOES) measurements are carried out with a Spectruma GDA 750 analyser in RF mode with a 4-mm anode.

3. Results and discussion

3.1 Electrochemical synthesis of PPy on iron in aqueous solution of sodium salicylate

Polypyrrole films are polymerized potentiostatically at 1.2 V vs. $Ag/AgCl_{sat}$ in the presence of 0.1 M sodium salicylate from solutions of 0.05, 0.1 or 0.15 M pyrrole. Figure 1 presents the typical chronoamperometric curves recorded during the polymer synthesis. It can be observed that the process of PPy formation is different depending on the pyrrole concentration.

Generally, the electropolymerization of pyrrole occurs in two steps. The first one is the iron passivation and the second is the PPy formation. At the beginning, the current density decreases due to the formation of the passivation layer [8,38]. After a certain time, the current

density starts to increase, indicating the beginning of the polymerization, and then it becomes stable, due to the steady state growth of polypyrrole.

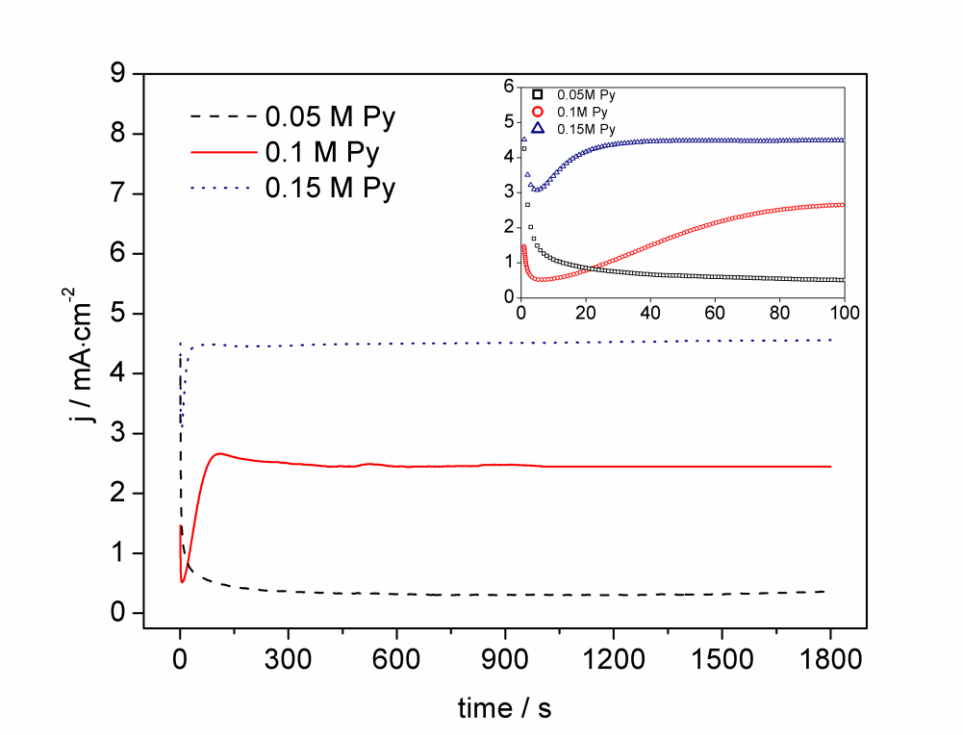

Figure 1. Chronoamperometric curves of the potentiostatic polymerization (1.2 V vs. $Ag/AgCl_{sat}$) of pyrrole on iron in aqueous solution of 0.1 M sodium salicylate and 0.05, 0.1 or 0.15 M pyrrole.

The two-step behaviour is clearly seen in the case of 0.1 and 0.15 M pyrrole. A higher initial value of the current density is found for the higher pyrrole concentration. The decrease in current density, corresponding to the metal passivation, and especially the subsequent increase, related to the polymerization, are faster for the higher monomer concentration. This all means that the electropolymerization process of pyrrole in the presence of higher concentration occurs more rapidly.

A different behaviour is seen for 0.05 M Py. The current density decreases monotonically and the PPy growth is not apparent in the chronoamperogram. This is caused by the too small amount of monomer available in the solution, which would involve the formation of a poor, thin polymeric layer.

3.2 Surface characterization of the PPy/Fe material

A cross-sectional SEM image of iron coated with polypyrrole (PPy/Fe) synthesized from a 0.1 M pyrrole solution is presented in Figure 2a. Three regions can be clearly seen: the polypyrrole film, the passivation interlayer and the iron substrate. It can be also noticed that the formed passivation interlayer is not uniformly formed on the metallic surface.

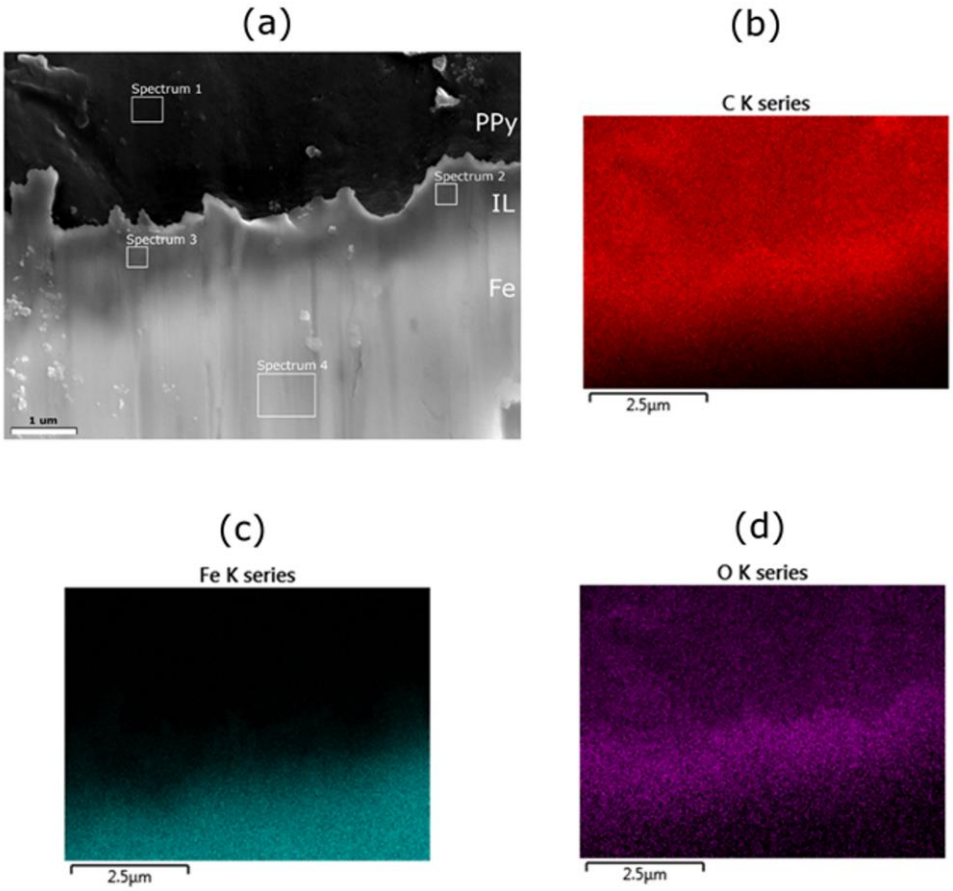

Figure 2. FE-SEM cross-sectional image of iron coated with PPy (a) and the corresponding EDX mapping images for C (b), Fe (c) and O (d).

In order to analyse the PPy/Fe material in more detail, EDX elemental mapping and spectral analysis are performed. EDX mapping images of carbon, iron and oxygen are presented in Figure 2. The brighter areas correspond to the presence of a higher amount of certain element in the cross-section of the PPy/Fe material. Figure 3 presents the chemical

analysis of C, Fe and O elements for the selected points on the cross-section of PPy/Fe, marked in Figure 2a.

The distribution of the carbon is the highest in the polymeric (~ 75 wt%) and interlayer (~ 68 wt%) regions, as seen in Figures 3a-c. The highest amount of iron is detected in the metallic substrate (95 wt%), in Figure 3d. The iron is also observed in the interlayer region (13-14 wt%) (Figures 3b-c) and almost no iron is observed in the polymeric layer (~ 1 wt%), in Figure 3a. Less iron content in the coating indicates good blocking properties of the passivating interlayer towards the iron dissolution [36]. As it can be seen, the incorporated oxygen is well distributed throughout the whole polymeric layer (~ 24 wt%). It means that the counter anions are incorporated quite homogenously in the PPy film. The oxygen is also present in the interlayer region (~ 18 wt%). The oxygen trace in the passivation layer is clearly seen in the mapping image (Figure 2d).

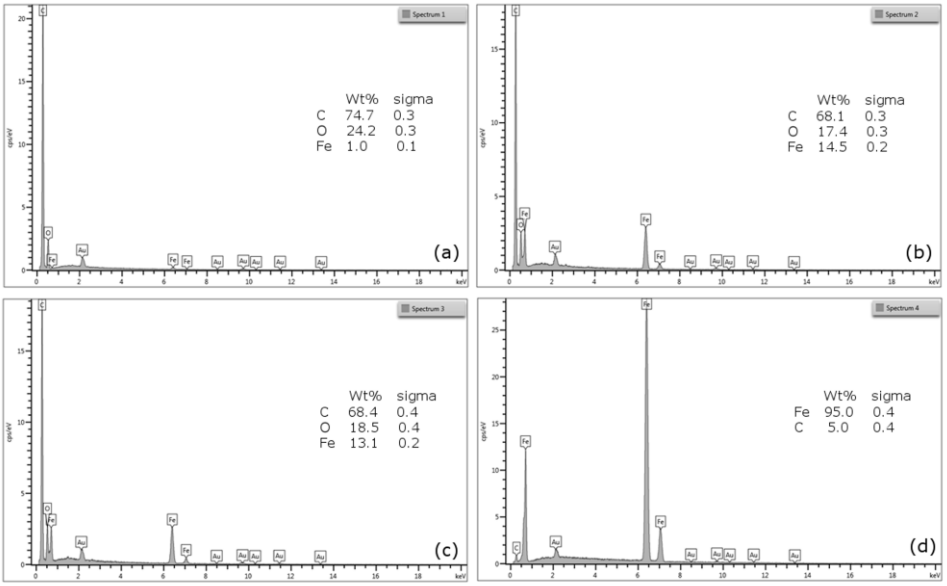

Figure 3. EDX elemental analysis of the selected points on the cross-section of PPy/Fe: polymeric film (a), interlayer (b,c) and iron substrate (d).

Glow discharge optical emission spectroscopy (GDOES) analysis is performed in order to study the composition profile of the PPy coated iron. Figure 4 presents the GDOES depth profile of carbon (C), oxygen (O) and iron (Fe) in the material.

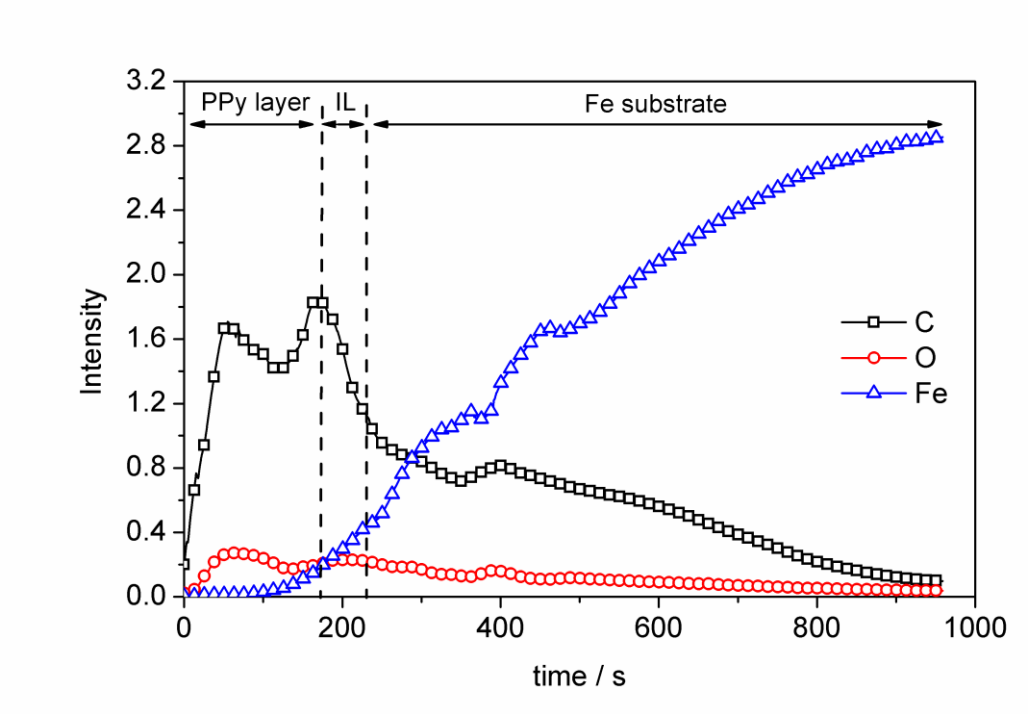

Figure 4. GDOES depth profiles of C, O and Fe of PPy/Fe synthesized in 0.1 M sodium salicylate and 0.1 M pyrrole at 1.2 V.

The elemental profiles reflect the transition from the PPy film to the iron substrate. The depth profiles show clear intensity variations of the C, O and Fe signals. Carbon and oxygen indicate the presence of the PPy film, iron is used as an indicator for the interlayer and metallic substrate, while the presence of the three elements relates to the interlayer. According to the elemental profiles, three regions could be distinguished in the material: the PPy layer with high content or carbon and a smaller amount of oxygen; the passivation layer between the PPy film and the substrate, corresponding to the gradual decrease of C content and increase of Fe content; and the iron substrate, with the contents of the C and O decreasing to zero and Fe being the dominant element. It must be noticed that, similarly to the results of the EDX analysis, virtually no iron can be observed in the polymeric layer. This indicates that the

passivation layer formed between iron and PPy, is stable and effectively inhibits the dissolution of iron.

The passivating properties of sodium salicylate and the appropriate selection of other parameters, such as concentration and deposition potential, result in the formation of a passivation interlayer (IL) directly on the iron surface, which is confirmed by the SEM, EDX and GDOES analyses. As a consequence, the dissolution of the metal becomes inhibited, which allows for the polypyrrole deposition. It is noticed that the main elements of the interlayer are carbon, oxygen and iron. Therefore, the layer might be a metallic salt such as iron-salicylate complex, as observed by others [32,39].

3.3 In-situ ORP-EIS study of the electrochemical synthesis of PPy on Fe

ORP-EIS measurements are performed to study quantitatively the electrochemical polymerization of pyrrole on iron in the presence of sodium salicylate. The electrochemical impedance spectra recorded during the electropolymerization of pyrrole from 0.05, 0.1 and 0.15 M pyrrole solutions are presented in Figures 5, 6 and 7, respectively.

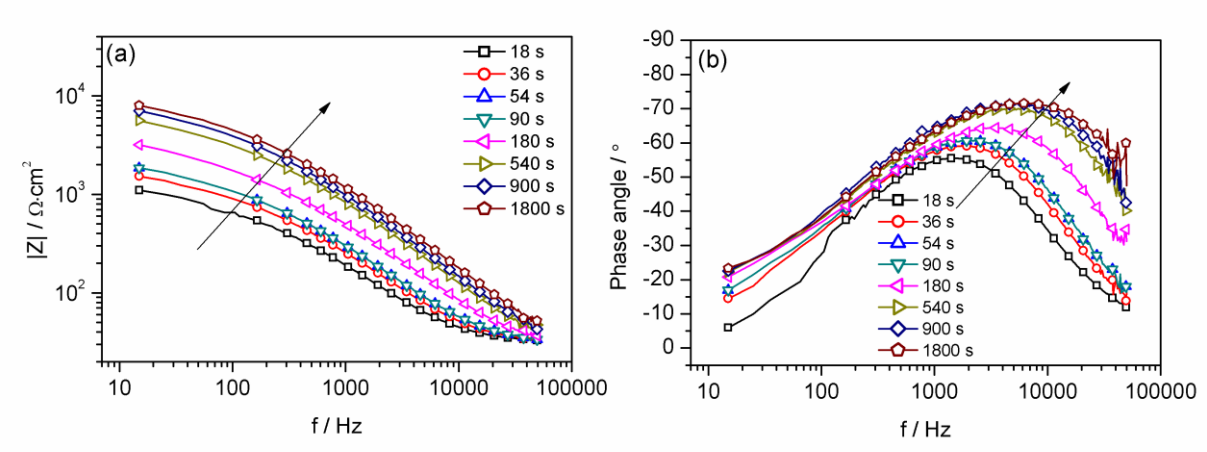

Figure 5. Bode modulus (a) and phase angle (b) plots of the impedance spectra recorded during the electropolymerization of pyrrole from a 0.1 M sodium salicylate and 0.05 M pyrrole solution at 1.2 V vs. $Ag/AgCl_{sat}$.

For all cases, the impedance modulus as well as the phase angle vary over the polymerization time. Moreover, it is clearly seen that the EIS behaviour depends strongly on the pyrrole concentration. In the case of 0.05 M Py, the impedance modulus increases continuously during the polymerization time (Figure 5a), although reaching a pseudo-stable state after 500 s. This observation is in line with the chronoamperometric curve in Figure 3. The shape of the EIS graphs shows resistive and capacitive contributions during the whole electropolymerization time.

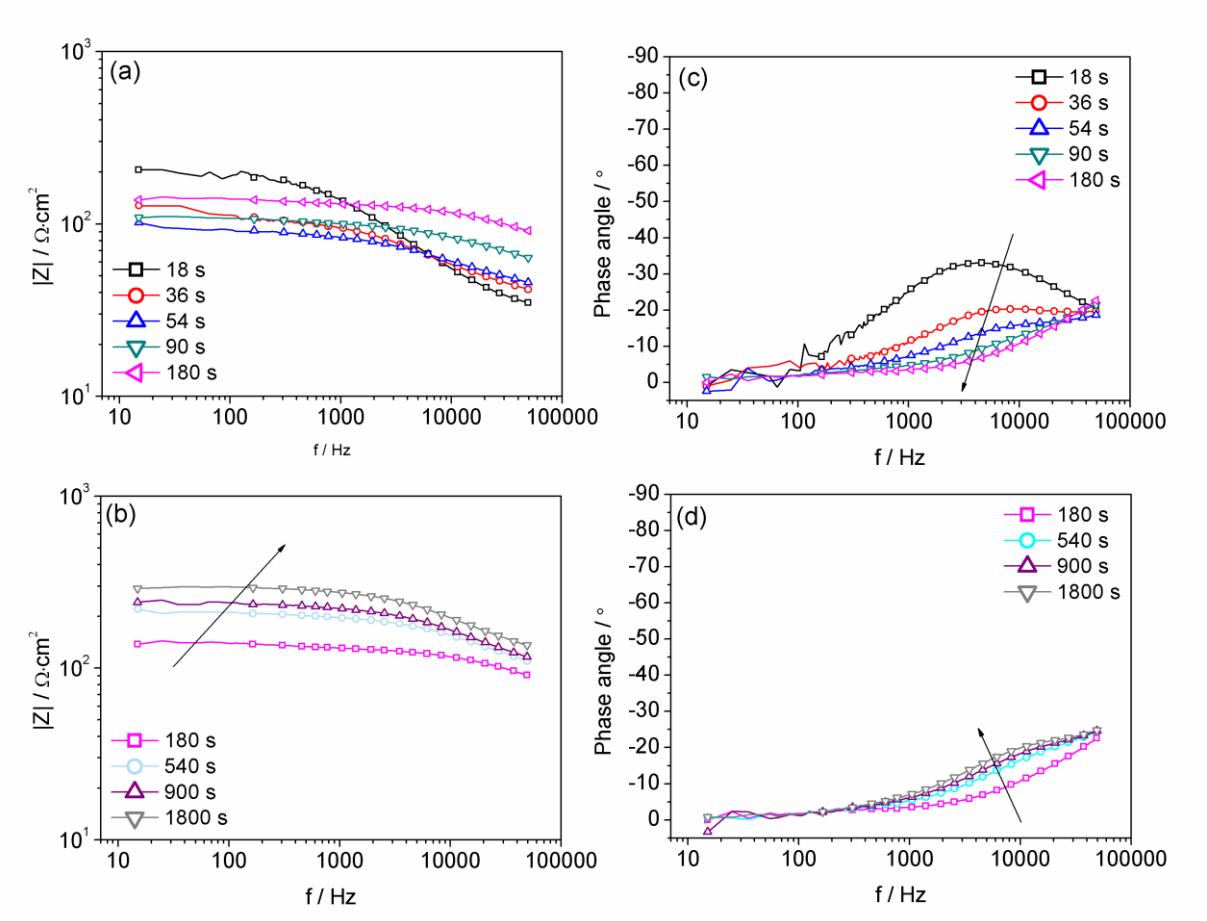

Figure 6. Bode modulus (a, b) and Bode phase angle (c, d) of the impedance spectra recorded during the electropolymerization of pyrrole from a 0.1 M sodium salicylate and 0.1 M pyrrole solution at 1.2 V vs. $Ag/AgCl_{sat}$.

For 0.1 M pyrrole, |Z| decreases at the beginning of the polymerization during the first minute and slightly increases afterwards (Figure 6a). After 180 s, the resistive behaviour is

predominant (Figures 6c and 6d) and the impedance slowly increases reaching a certain stability after 900 s, as observed in section 3.1. In the case of 0.15 M pyrrole, |Z| increases during the whole synthesis time (Figure 7). Here, the strong contribution of the resistive processes can be observed. The impedance behaviour is similar to the one observed for 0.1 M Py, yet the stability of the system is reached faster.

In general, it can be seen that the impedance modulus is lower with increasing pyrrole concentration. This indicates that a higher monomer concentration provides more effective electropolymerization of pyrrole on iron, which is also observed in the higher current density of chronoamperometric curve (Figure 1). For 0.05, 0.1 and 0.15 M Py, the change in |Z| is faster at the beginning of the electropolymerization and, with time, it becomes relatively stable.

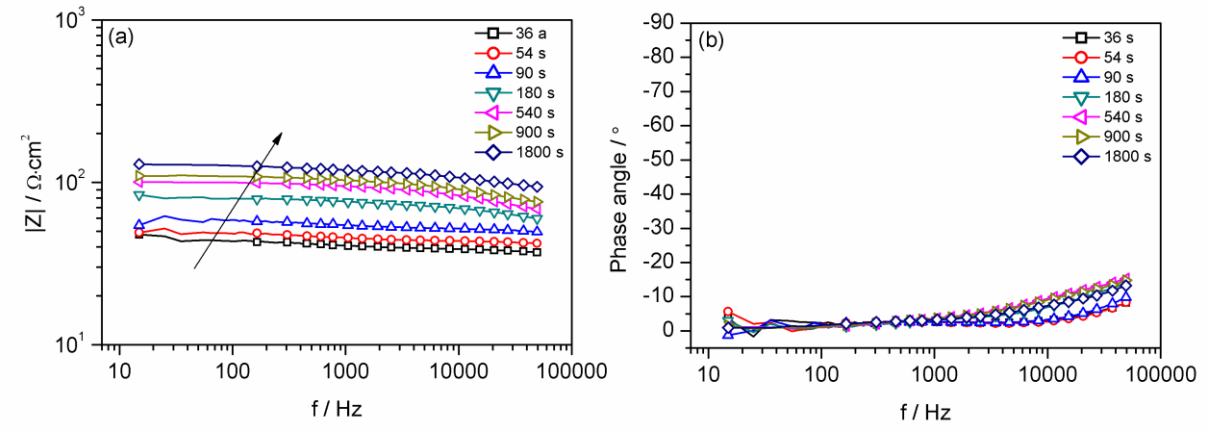

Figure 7. Bode modulus (a) and phase angle (b) plots of the impedance spectra recorded during the electropolymerization of pyrrole from a 0.1 M sodium salicylate and 0.15 M pyrrole solution at 1.2 V vs. $Ag/AgCl_{sat}$.

3.4 Reliability of the experimental data

The modelling of the EIS data can only be performed if the conditions of linearity and stationarity are met [52].

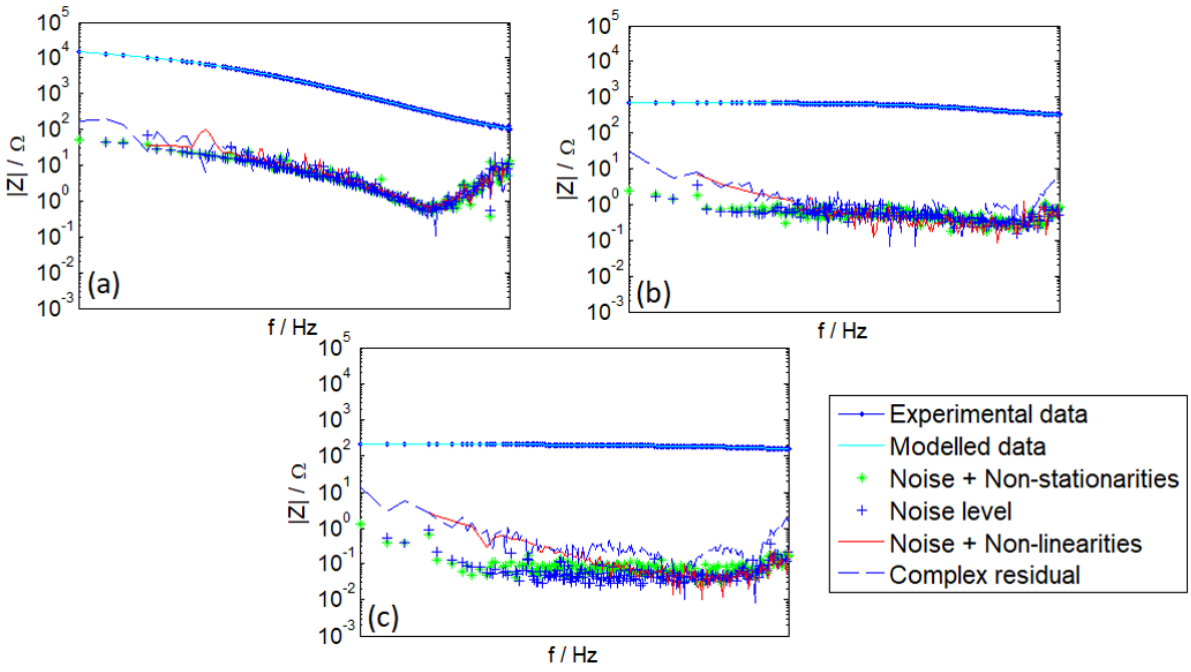

Figure 8. Experimental and modelled impedance and noise levels during the electropolymerization process from 0.05 M (a), 0.1 M (b) and 0.15 M (c) pyrrole solutions.

The quality of the experimental data can be assessed by the analysis of the levels of noise, non-linearities and non-stationarities of the studied system, which are provided with an ORP-EIS measurement. The curve of the noise level and non-linearities must overlap the noise level to have a linear behaviour. For a stationary behaviour, the noise level and the curve of the noise level and non-stationarities must not differ [49–51].

In Figure 8, the experimental curves and noise levels are presented for selected EIS spectra during the PPy electropolymerization using different monomer concentrations. It can be seen that all curves related to the noise level, non-stationarities and non-linearities coincide for all cases. Besides, the signal-to-noise ratio is, in general, two orders of magnitude. Similar characteristics are obtained for the whole recorded dataset. It proves that the EIS data are measured preserving the conditions of linearity and stationarity, which confirms the reliability of the data.

3.5 Modelling of the impedance data: fitting and estimation of the EEC parameters

Once the quality of the experimental data is confirmed, the modelling can be performed. Figures 9a and 9b present the equivalent electrical circuits used to model the impedance data of the PPy electrosynthesis using 0.1 M and 0.15 M pyrrole (circuit 1) and 0.05 M pyrrole (circuit 2).

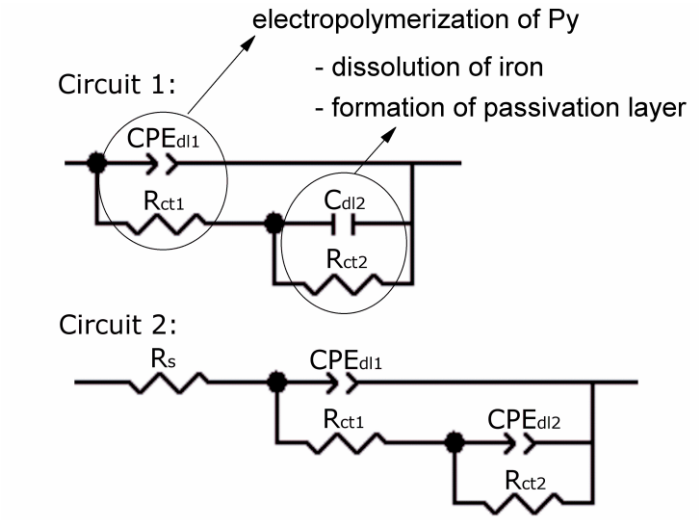

Figure 9. Equivalent electrical circuits used to model the ORP-EIS experiments for 0.15 and 0.1 M (circuit 1), and 0.05 M (circuit 2) pyrrole.

In the proposed equivalent circuits, the time constant CPE_{dl1}-R_{ct1} corresponds to the electropolymerization reaction. It is characterized by R_{ct1}, the charge transfer resistance of the polymerization reaction, which can be associated with the monomer oxidation and/or polymer deposition on the iron electrode, and CPE_{dl1}, the constant phase element of the double layer associated with the polymerization reaction. The C_{dl2}-R_{ct2} component is related to the reactions occurring on the iron substrate and/or between the metal and the polymer; these might be the dissolution of iron; formation of the passivation interlayer and/or other oxidation/reduction reactions present in the system. These processes are described by the charge transfer resistance R_{ct2} and the double layer capacitance C_{dl2}. It must be noticed that the solution resistance is not included in the circuit 1 since its contribution is masked by the CPE_{dl1}-R_{ct1} contribution at high frequencies.

In the case of 0.05 M pyrrole, the proposed equivalent electrical circuit 1 insufficiently reflects the measurements. Therefore, an alternative circuit 2 is used, where a solution resistance R_s is added and C_{dl2} is replaced by CPE_{dl2}.

A constant phase element (CPE) is commonly used instead of a pure capacitor to compensate the inhomogeneities and non-ideal capacitive behaviour of conducting polymer modified electrodes [9,53]. The impedance of a constant phase element Z_{CPE} is formulated with the following general equation:

$$Z_{CPE} = 1/Q(j\omega)^{\alpha} \quad (1)$$

When α = 1, the CPE represents the ideal capacitor and Q corresponds to the capacitance. When $0 < \alpha < 1$, the system shows a behaviour attributed to the material heterogeneity. Here, the use of CPE_{dl1} and CPE_{dl2} provides a better match between model and experiment for the whole dataset, with values of α_1 and α_2 lower than 1, which exclude the use of a pure capacitor.

The results of the modelling for each monomer concentration are presented in Figure 8; the modelled data and modelling residuals are shown together with the experimental data. The modelled impedance curves match adequately the experimental curves. Yet, to properly assess the quality of the modelling, the complex residual is compared to the noise level. It can be observed that for each pyrrole concentration, the residual overlaps the noise level almost in the entire frequency range. A good agreement between experiment and model is obtained for the whole datasets. This indicates the statistical validity of the proposed models.

The circuit parameters and their standard deviations are determined for every experiment. The evolution of the resistive and capacitive parameters over time is presented in Figures 10-11 with the errors bars representing the parameter standard deviations. The parameter values are given with regard to the geometrical area of the electrode.

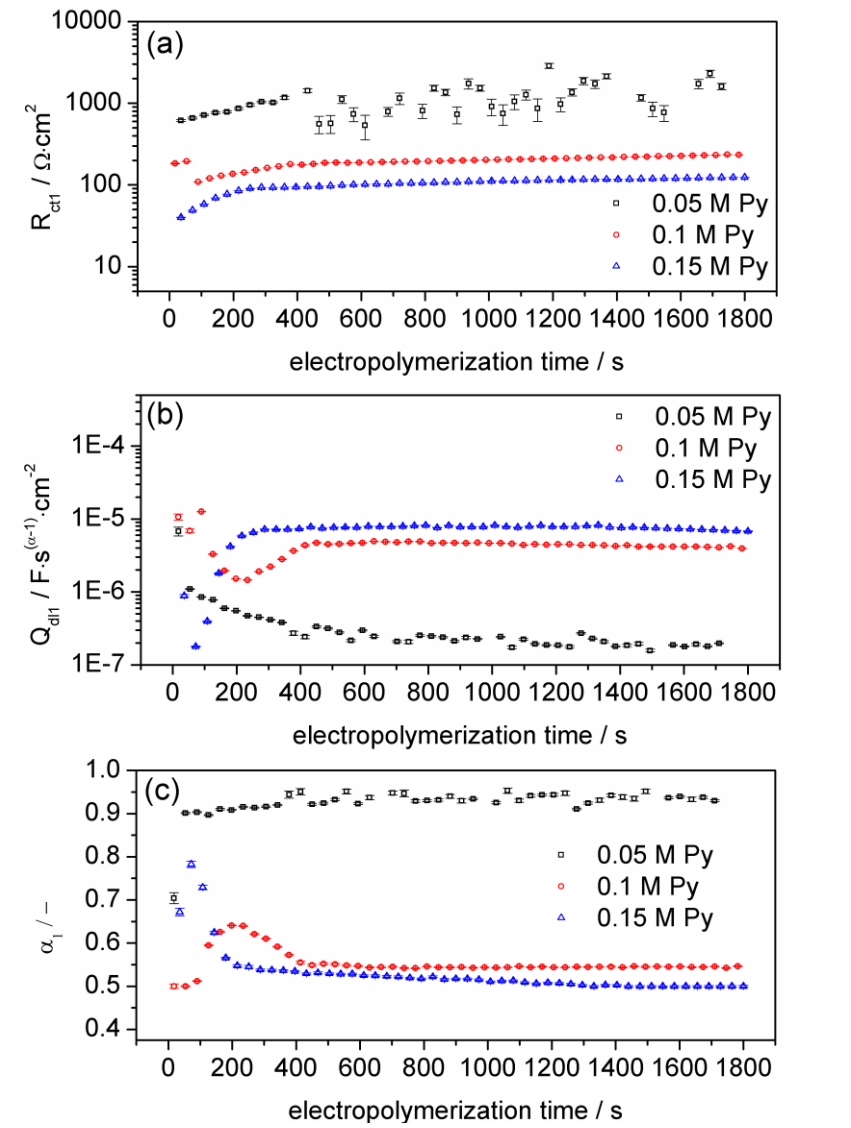

Figure 10. Evolution of the R_{ct1} (a), Q_{dl1} (b) and α_1 (c) parameters over the electropolymerization time for different pyrrole concentrations.

The evolution of the R_{ct1} and Q_{dl1} parameters related to the polymerization process can be seen in Figures 10a and 10b, respectively. Their behaviour is strongly dependent on the pyrrole concentration. The charge transfer resistance for all pyrrole concentrations increases at the beginning of the polymerization. This increase suggests that the electropolymerization process is more difficult at the start. This can be due to the iron passivation process. Once the surface of the iron is ready, the PPy deposition occurs more effectively and, after a certain time, it gets to a steady state. Indeed, the values of R_{ct1} become constant, reaching a plateau for 0.1 and 0.15 M Py around 190 Ω·cm^2 and 100 Ω·cm^2, respectively and a pseudo-plateau

for 0.05 M Py around 1500 $\Omega \cdot cm^2$. Some fluctuations of the resistance can be observed in the case of 0.05 M Py, which can be due to the inhibited deposition process of polypyrrole. The slight increase of R_{ct1} observed towards the end of the experiment might be due to the overoxidation of the PPy layer, which, being less conducting, would partially inhibit the deposition reactions.

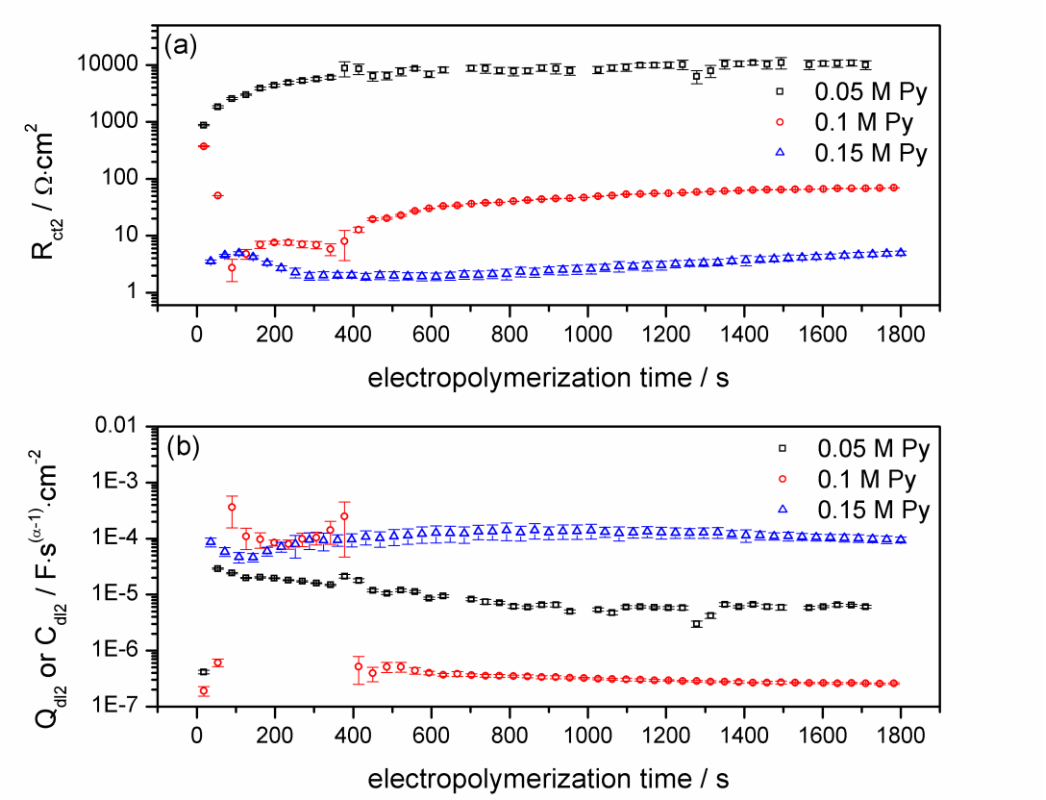

Figure 11. Evolution of the R_{ct2} (a) and Q_{dl2} or C_{dl2} (b) parameters over the electropolymerization time for different pyrrole concentrations.

The stability of the PPy deposition is obtained faster for the higher pyrrole concentration. It can be also noticed that the values of the charge transfer resistance of the polymerization process are higher for the lower pyrrole concentration. This is related to the fact that a higher monomer concentration makes the polymerization of pyrrole easier to proceed. This behaviour could already be anticipated from the ORP-EIS spectra at high frequencies (Figures 5, 6, 7) and the chronoamperometric curves (Figure 1) recorded during the PPy electrodeposition.

The evolution of Q_{dl1} also strongly depends on the pyrrole concentration (Figure 10b). For 0.1 and 0.15 M the trend of the capacitive component is very similar. The decrease in Q_{dl1} is observed at the beginning of the synthesis process. Then, its value increases, and it stabilizes after approximately 400 s and 200 s, respectively. The changes in the capacitive component results from the variation of the active surface area of the electrode assuming a similar correlation as for a pure capacitor, according to:

$$C = \varepsilon_o \varepsilon_r A/d \quad (2)$$

where ε_o is the vacuum permittivity, ε_r is the relative permittivity, A is the surface area and d is the thickness of the double layer.

The decrease of Q_{dl1} might suggest that the synthesis process starts: the emerging interlayer prepares the iron surface for the PPy deposition. The passivation layer, acting as first as a barrier, would block the reactive iron surface, decreasing the initial active area. Yet, the development of the interlayer allows for the further PPy deposition by the inhibition of the iron dissolution. After a certain time, Q_{dl1} rises, due to the increase of the electrode surface area, a fact that is well known for the conducting polymers films [53,54]. This corresponds to the start of the active deposition of PPy on the modified iron. After a while, Q_{dl1} stabilizes, which indicates that the surface area of the forming material does not change significantly. This, in turn, suggests that the electropolymerization process of pyrrole under the applied conditions proceeds in a stable way. The stabilization of Q_{dl1} is reached faster for higher pyrrole concentrations. This finding is compatible with the chronoamperometric study and the trend of the corresponding resistance component R_{ct1}.

A different behaviour can be seen in the case of 0.05 M Py. Here, the value of Q_{dl1} decreases at the beginning due to the coverage of the electrode by the interlayer and then it becomes approximately constant. No increase of Q_{dl1} is observed as the polymerization

proceeds. This indicates that almost no PPy layer is formed on the iron under the applied condition [20,54].

Besides, it can be observed that the value of Q_{dl1} is higher for higher monomer concentrations. More amount of the monomer in the synthesis solution allows for easier PPy formation [8]: the higher Q_{dl1} is due to the higher surface area obtained for the synthesized PPy.

The evolution of α_1 related to the CPE_{dl1} component is presented in Figure 10c. As for R_{ct1} and Q_{dl1}, α_1 differs depending on the monomer concentration. The trend is similar for 0.1 and 0.15 M Py. Firstly, the value of α_1 increases, then it decreases and becomes constant. These transitions are faster in the case of 0.15 M Py, similarly to the evolution of Q_{dl1}. The increase of α_1 can be related to the formation of the interlayer. The formed interlayer makes the interface more homogenous at first, which results in a higher α_1. However, the decrease of α_1 indicates the beginning of the active PPy deposition, which makes the electrode more porous. α_1 stabilizes faster for 0.15 M Py than for 0.1 M Py with values around 0.5 and 0.55, respectively. For conducting polymers, the variation of the α parameter below 1 can be linked to a material distribution of properties, related to the material roughness and the porosity of the films [53,55]. The α_1 values around 0.5 correspond to the special case of active porous electrode, which has also been observed in the case of polyaniline (PANI) electrodeposited on a platinum electrode [48]. Therefore, it can be suggested that the PPy film synthesized with a higher monomer concentration results in the formation of a polymeric film with higher heterogeneities or porosity.

The α_1 parameter for the lowest pyrrole concentration, 0.05 M Py, reveals a trend different to the other cases. Here, α_1 increases immediately after the electropolymerization process starts and then it remains constant with a value around 0.9 until the end of the process.

This can be related to the fact that a passivation process dominates under this condition, which finally would result in the formation of a thin and smooth (less porous) PPy layer.

The evolution of the R_{ct2} and Q_{dl2} or C_{dl2} elements can be seen in Figures 11a and 11b, respectively. The R_{ct2}-Q_{dl2}/C_{dl2} time constant is believed to reflect different reactions that occur on the surface of iron and/or between iron/polypyrrole. These reactions would be the dissolution of iron, the passivation process, which immediately inhibits the metal dissolution, and the formation of the interlayer, which allows for the PPy electrodeposition.

From Figure 11, it can be clearly seen that all parameters are influenced by the pyrrole concentration. Thus, the reactions represented by R_{ct2}-Q_{dl2}/C_{dl2} are associated with the polymerization process of pyrrole and depend also on the synthesis conditions.

R_{ct2} decreases with increasing monomer concentration, that is, the processes at intermediate frequencies proceed easier in the case of the higher monomer concentration, whereas they are inhibited when the pyrrole concentration is too low. Overall the evolution of R_{ct2} is similar to the one observed for the high frequency resistive component R_{ct1}. For 0.15 M Py, R_{ct2} increases slightly first, then it decreases and for most of the polymerization time it remains constant with a value of 2 $\Omega \cdot cm^2$; later on, it increases slightly to the end of the synthesis process. In the case of 0.1 M Py, R_{ct2} decreases at the beginning, then it increases and after then it remains almost constant around 55 $\Omega \cdot cm^2$. In the case of 0.05 M Py, R_{ct2} increases up to approximately 10 $k\Omega \cdot cm^2$ and then it remains more or less constant. In a similar way as for the electropolymerization reactions (at high frequencies), insufficient amount of pyrrole might hinder the reactions associated with the formation of the interlayer and/or the iron/polymer interactions.

The different stages of the R_{ct2} evolution before the steady-state are related to: 1) the iron dissolution, not visible for 0.15 M due to the faster time-scale of the processes; 2) the iron passivation; 3) the formation of the interlayer.

The constant values of R_{ct2} achieved after a certain time show that the occurring processes become stable. The reincrease observed for 0.15 M at the end of the deposition time is due to the fact that the synthesis process is much faster with the higher pyrrole concentrations. This might result in the formation of a too thick PPy layer, which starts to block the reactions occurring in the PPy/Fe interface.

Figure 11b presents the evolution of the corresponding Q_{dl2} or C_{dl2}. The fast increase of C_{dl2} and Q_{dl2} at the beginning of the synthesis process is observed in the case of 0.1, 0.15 and 0.05 M Py, respectively. Then, there is a variation of parameters, and finally it becomes almost constant. An additional drop is seen in the case of 0.1 M pyrrole before the stabilization. The variations of C_{dl2} and Q_{dl2} might suggest that the surface and interface available for the oxidation/reduction reactions of the formation of the interlayer are changing [47]. Over time the processes stabilize and reach the steady-state. This might be associated with the growth of a well formed PPy layer that stabilizes the reactions at PPy/Fe interface.

The α_2 parameter for 0.05 M pyrrole is around 0.5 during all electropolymerization process, which is due to the high heterogeneity of the iron interface. The chronoamperogram in Figure 1 shows the low extension of the Py deposition on the iron. Besides, the poorly deposited PPy layer does not allow the formation of a stable and proper covering interlayer on the iron surface. These phenomena result in the distribution of the low-frequency processes related to the PPy/Fe interface reactions.

To model the processes occurring with 0.1 and 0.15 M Py a pure capacitor C_{dl2} is used. This might be a proof that the R_{ct2}-C_{dl2} time constant is not directly related to the formation of the PPy layer on iron. As it is mentioned in literature [9,53] the synthesized PPy film has a very high porous and heterogeneous structure, which very often excludes the use of a pure capacitor.

Based on the analysed results it is evident that the electrosynthesis process of pyrrole on oxidizable iron in the presence of sodium salicylate is a complex process. It includes not only the oxidation of pyrrole but also reactions such as the oxidation/reduction of the iron surface and/or reactions between the iron, formed interlayer and polypyrrole. It differs from the electropolymerization on noble metals such as platinum, where direct deposition of pyrrole occurs [56]. The impedance measurements and modelling suggest that the formation of the interlayer and/or other oxidation/reduction reactions, such as the dissolution and passivation of iron, are influenced by the monomer concentration during the electropolymerization process. The role of the interlayer is crucial in the electrosynthesis process, since it inhibits the activity of the reactive metallic substrate and allows for the stable PPy deposition. The latter is confirmed by the constant current recorded during the polymer electrosynthesis and the steady-state behaviour of the parameters determined by the EIS modelling.

4. Conclusions

The electrochemical synthesis of polypyrrole on iron in aqueous solution of pyrrole and sodium salicylate has been successfully studied in-situ by ORP-EIS for the first time. The PPy/Fe material has been also analysed with the SEM, EDX and GDOES. The results confirm the passivating properties of sodium salicylate. It is shown that a passivation interlayer is formed directly on iron prior to the PPy deposition under certain synthesis parameters, such as concentration and deposition potential. It is noticed that the main elements of the interlayer are carbon, oxygen and iron, which indicates that the layer might be a metallic salt such as iron-salicylate complex.

The ORP-EIS study provides a reliable analysis of the electrosynthesis of PPy on iron depending on the pyrrole concentration. It is shown that the concentration of monomer strongly influences the electrosynthesis process of polypyrrole on iron. It is proven that electropolymerization of the polymer on oxidizable metal includes at least two processes,

which are not seen in the case of noble metals. The first process is assigned to the monomer oxidation/polymer deposition, while the second one is associated with the oxidation/reduction of the iron surface and/or reactions between the iron, formed interlayer and polypyrrole. The evolution of these processes is discussed as a function of the polymerization time. The present study shows that both the PPy deposition reactions and the iron interface reactions are influenced by the monomer concentration.

Acknowledgements

This work was supported by the National Science Centre (Poland) ["Preludium" grant based on the decision 2016/23/N/ST5/00346] and by the Faculty of Electronics, Telecommunications and Informatics, Gdansk University of Technology [Statutory Funds], within a joint PhD programme with Vrije Universiteit Brussel.

The GDOES measurements are performed at OnderzoeksCentrum voor Aanwending van Staal (OCAS) with the help of Barbara Van Langenhove. The authors would like to thank Priya Laha for the FE-SEM/EDX analysis.

References

[1] Y.F. Zheng, X.N. Gu, F. Witte, Biodegradable metals, Mater. Sci. Eng. R. 77 (2014) 1–34. doi:10.1016/J.MSER.2014.01.001.

[2] M. Moravej, D. Mantovani, Biodegradable metals for cardiovascular stent application: interests and new opportunities, Int. J. Mol. Sci. 12 (2011) 4250–4270. doi:10.3390/ijms12074250.

[3] A. Francis, Y. Yang, S. Virtanen, A.R. Boccaccini, Iron and iron-based alloys for temporary cardiovascular applications, J. Mater. Sci. Mater. Med. 26 (2015) 1–16. doi:10.1007/s10856-015-5473-8.

[4] J. He, F.-L. He, D.-W. Li, Y.-L. Liu, Y.-Y. Liu, Y.-J. Ye, D.-C. Yin, Advances in Fe-based biodegradable metallic materials, RSC Adv. 6 (2016) 112819–112838.

doi:10.1039/C6RA20594A.

[5] D. Sun, Y. Zheng, T. Yin, C. Tang, Q. Yu, G. Wang, Coronary drug-eluting stents: From design optimization to newer strategies, J. Biomed. Mater. Res. Part A. 102 (2014) 1625–1640. doi:10.1002/jbm.a.34806.

[6] F. Singer, D. Rückle, M.S. Killian, M.C. Turhan, S. Virtanen, Electropolymerization and Characterization of Poly-N- methylpyrrole Coatings on AZ91D Magnesium Alloy, Int. J. Electrochem. Sci. 8 (2013) 11924–11932. www.electrochemsci.org (accessed April 17, 2018).

[7] Z. Grubač, I.Š. Rončević, M. Metikoš-Huković, Corrosion properties of the Mg alloy coated with polypyrrole films, Corros. Sci. 102 (2016) 310–316. doi:10.1016/J.CORSCI.2015.10.022.

[8] K. Włodarczyk, F. Singer, P. Jasiński, S. Virtanen, Solid State Conductivity of Optimized Polypyrrole Coatings on Iron Obtained from Aqueous Sodium Salicylate Solution Determined by Impedance Spectroscopy, Int. J. Electrochem. Sci. 9 (2014) 7997–8010. www.electrochemsci.org (accessed April 17, 2018).

[9] K. Cysewska, L.F. Macía, P. Jasiński, A. Hubin, Tailoring the electrochemical degradation of iron protected with polypyrrole films for biodegradable cardiovascular stents, Electrochim. Acta. 245 (2017) 327–336. doi:10.1016/j.electacta.2017.05.172.

[10] G. Inzelt, Conducting polymers: a new era in electrochemistry, Springer, 2012.

[11] L.-X. Wang, X.-G. Li, Y.-L. Yang, Preparation, properties and applications of polypyrroles, React. Funct. Polym. 47 (2001) 125–139. doi:10.1016/S1381-5148(00)00079-1.

[12] D. Nguyen, H. Yoon, Recent Advances in Nanostructured Conducting Polymers: from Synthesis to Practical Applications, Polymers (Basel). 8 (2016) 1–38. doi:10.3390/polym8040118.

[13] D.D. Ateh, H.A. Navsaria, P. Vadgama, Polypyrrole-based conducting polymers and interactions with biological tissues, J. R. Soc. Interface. 3 (2006) 741–52. doi:10.1098/rsif.2006.0141.

[14] M.B. González, S.B. Saidman, Corrosion protection properties of polypyrrole electropolymerized onto steel in the presence of salicylate, Prog. Org. Coatings. 75 (2012) 178–183. doi:10.1016/J.PORGCOAT.2012.04.015.

[15] B.. Grgur, N.. Krstajić, M.. Vojnović, Č. Lačnjevac, L. Gajić-Krstajić, The influence of polypyrrole films on the corrosion behavior of iron in acid sulfate solutions, Prog. Org. Coatings. 33 (1998) 1–6. doi:10.1016/S0300-9440(97)00112-4.

[16] I. Gualandi, L. Guadagnini, S. Zappoli, D. Tonelli, A Polypyrrole Based Sensor for the Electrochemical Detection of OH Radicals, Electroanalysis. 26 (2014) 1544–1550. doi:10.1002/elan.201400054.

[17] K. Cysewska, J. Karczewski, P. Jasiński, Recurrent potential pulse technique for improvement of glucose sensing ability of 3D polypyrrole, Meas. Sci. Technol. 28 (2017) 074004 1-10. doi:10.1088/1361-6501/aa6f8f.

[18] C.C. Bof Bufon, T. Heinzel, Polypyrrole thin-film field-effect transistor, Appl. Phys. Lett. 89 (2006) 012104. doi:10.1063/1.2219375.

[19] A. Madhan Kumar, N. Rajendran, Electrochemical aspects and in vitro biocompatibility of polypyrrole/TiO2 ceramic nanocomposite coatings on 316L SS for orthopedic implants, Ceram. Int. 39 (2013) 5639–5650. doi:10.1016/J.CERAMINT.2012.12.080.

[20] K. Cysewska, J. Karczewski, P. Jasiński, Electrochemical synthesis of 3D nano-/micro-structured porous polypyrrole, Mater. Lett. 183 (2016) 397–400. doi:10.1016/j.matlet.2016.07.154.

[21] J. Ouyang, Y. Li, Effect of electrolyte solvent on the conductivity and structure of as-

prepared polypyrrole films, Polymer (Guildf). 38 (1997) 1971–1976. doi:10.1016/S0032-3861(96)00749-5.

[22] K. Cysewska, S. Virtanen, P. Jasiński, Study of the electrochemical stability of polypyrrole coating on iron in sodium salicylate aqueous solution, Synth. Met. 221 (2016) 1–7. doi:10.1016/j.synthmet.2016.09.022.

[23] S. Demoustier-Champagne, P.-Y. Stavaux, Effect of Electrolyte Concentration and Nature on the Morphology and the Electrical Properties of Electropolymerized Polypyrrole Nanotubules, Chem. Mater. 11 (1999) 829–834. doi:10.1021/CM9807541.

[24] C.C.B. Bufon, T. Heinzel, P. Espindola, J. Heinze, Influence of the Polymerization Potential on the Transport Properties of Polypyrrole Films, J. Phys. Chem. B. 114 (2010) 714–718. doi:10.1021/JP908565Y.

[25] K.M. Cheung, D. Bloor, G.C. Stevens, Characterization of polypyrrole electropolymerized on different electrodes, Polymer (Guildf). 29 (1988) 1709–1717. doi:10.1016/0032-3861(88)90288-1.

[26] S. Biallozor, A. Kupniewska, Conducting polymers electrodeposited on active metals, Synth. Met. 155 (2005) 443–449. doi:10.1016/J.SYNTHMET.2005.09.002.

[27] T. Zalewska, A. Lisowska-Oleksiak, S. Biallozor, V. Jasulaitiene, Polypyrrole films polymerised on a nickel substrate, Electrochim. Acta. 45 (2000) 4031–4040. doi:10.1016/S0013-4686(00)00497-7.

[28] J. Petitjean, J. Tanguy, J.C. Lacroix, K.I. Chane-Ching, S. Aeiyach, M. Delamar, P.C. Lacaze, Interpretation of the ultra-fast electropolymerization of pyrrole in aqueous media on zinc in a one-step process: The specific role of the salicylate salt investigated by X-ray photoelectron spectroscopy (XPS) and by electrochemical quartz crystal microba, J. Electroanal. Chem. 581 (2005) 111–121. doi:10.1016/J.JELECHEM.2005.04.024.

[29] T. Tüken, Polypyrrole films on stainless steel, Surf. Coatings Technol. 200 (2006) 4713–4719. doi:10.1016/J.SURFCOAT.2005.04.011.

[30] F. Beck, R. Michaelis, F. Schloten, B. Zinger, Filmforming electropolymerization of pyrrole on iron in aqueous oxalic acid, Electrochim. Acta. 39 (1994) 229–234. doi:10.1016/0013-4686(94)80058-8.

[31] Y.. Jiang, X.. Guo, Y.. Wei, C.. Zhai, W.. Ding, Corrosion protection of polypyrrole electrodeposited on AZ91 magnesium alloys in alkaline solutions, Synth. Met. 139 (2003) 335–339. doi:10.1016/S0379-6779(03)00181-4.

[32] A. Srinivasan, P. Ranjani, N. Rajendran, Electrochemical polymerization of pyrrole over AZ31 Mg alloy for biomedical applications, Electrochim. Acta. 88 (2013) 310–321. doi:10.1016/J.ELECTACTA.2012.10.087.

[33] W. Prissanaroon, N. Brack, P.J. Pigram, J. Liesegang, A surface and electrochemical study of polypyrrole coated on stainless steel and copper, Curr. Appl. Phys. 4 (2004) 163–166. doi:10.1016/J.CAP.2003.10.022.

[34] A.C. Cascalheira, S. Aeiyach, P.C. Lacaze, L.M. Abrantes, Electrochemical synthesis and redox behaviour of polypyrrole coatings on copper in salicylate aqueous solution, Electrochim. Acta. 48 (2003) 2523–2529. doi:10.1016/S0013-4686(03)00295-0.

[35] H. Nguyen Thi Le, B. Garcia, C. Deslouis, Q. Le Xuan, Corrosion protection of iron by polystyrenesulfonate-doped polypyrrole films, J. Appl. Electrochem. 32 (2002) 105–110. doi:10.1023/A:1014273624807.

[36] N.T.L. Hien, B. Garcia, A. Pailleret, C. Deslouis, Role of doping ions in the corrosion protection of iron by polypyrrole films, Electrochim. Acta. 50 (2005) 1747–1755. doi:10.1016/J.ELECTACTA.2004.10.072.

[37] T. Van Schaftinghen, S. Joiret, C. Deslouis, H. Terryn, In situ Raman Spectroscopy and Spectroscopic Ellipsometry Analysis of the Iron/Polypyrrole Interface, J. Phys. Chem.

C. 111 (2007) 14400–14409. doi:10.1021/JP0734878.

[38] S. Wencheng, J.O. Iroh, Electrodeposition mechanism of polypyrrole coatings on steel substrates from aqueous oxalate solutions, Electrochim. Acta. 46 (2000) 1–8. doi:10.1016/S0013-4686(00)00518-1.

[39] A. El Jaouhari, A. El Asbahani, M. Bouabdallaoui, Z. Aouzal, D. Filotás, E.A. Bazzaoui, L. Nagy, G. Nagy, M. Bazzaoui, A. Albourine, D. Hartmann, Corrosion resistance and antibacterial activity of electrosynthesized polypyrrole, Synth. Met. 226 (2017) 15–24. doi:10.1016/J.SYNTHMET.2017.01.008.

[40] J.. Martins, M. Bazzaoui, T.. Reis, E.. Bazzaoui, L. Martins, Electrosynthesis of homogeneous and adherent polypyrrole coatings on iron and steel electrodes by using a new electrochemical procedure, Synth. Met. 129 (2002) 221–228. doi:10.1016/S0379-6779(02)00057-7.

[41] A.A. Hermas, M. Nakayama, K. Ogura, Formation of stable passive film on stainless steel by electrochemical deposition of polypyrrole, Electrochim. Acta. 50 (2005) 3640–3647. doi:10.1016/J.ELECTACTA.2005.01.005.

[42] K. Cysewska, S. Virtanen, P. Jasiński, Electrochemical activity and electrical properties of optimized polypyrrole coatings on iron, J. Electrochem. Soc. 162 (2015) E307–E313. doi:10.1149/2.0821512jes.

[43] K. Cysewska, M. Gazda, P. Jasiński, Influence of electropolymerization temperature on corrosion, morphological and electrical properties of PPy doped with salicylate on iron, Surf. Coatings Technol. 328 (2017) 248–255. doi:10.1016/j.surfcoat.2017.08.055.

[44] S. Chaudhari, S.R. Sainkar, P.P. Patil, Anticorrosive properties of electrosynthesized poly(o-anisidine) coatings on copper from aqueous salicylate medium, J. Phys. D. Appl. Phys. 40 (2007) 520–533. doi:10.1088/0022-3727/40/2/028.

[45] J. Tietje-Girault, C. Ponce de León, F.C. Walsh, Electrochemically deposited

polypyrrole films and their characterization, Surf. Coatings Technol. 201 (2007) 6025–6034. doi:10.1016/J.SURFCOAT.2006.11.009.

[46] N.M. Martyak, Chronoamperometric studies during the polymerization of aniline from an oxalic acid solution, Mater. Chem. Phys. 81 (2003) 143–151. doi:10.1016/S0254-0584(03)00167-6.

[47] G.S. Popkirov, E. Barsoukov, R.N. Schindler, Investigation of conducting polymer electrodes by impedance spectroscopy during electropolymerization under galvanostatic conditions, J. Electroanal. Chem. 425 (1997) 209–216. doi:10.1016/S0022-0728(96)04965-0.

[48] R. Schrebler, H. Gómez, R. Córdova, L.M. Gassa, J.R. Vilche, Study of the aniline oxidation process and characterization of Pani films by electrochemical impedance spectroscopy, Synth. Met. 93 (1998) 187–192. doi:10.1016/S0379-6779(97)04107-6.

[49] Y. Van Ingelgem, E. Tourwé, O. Blajiev, R. Pintelon, A. Hubin, Advantages of Odd Random Phase Multisine Electrochemical Impedance Measurements, Electroanalysis. 21 (2009) 730–739. doi:10.1002/elan.200804471.

[50] E. Van Gheem, R. Pintelon, J. Vereecken, J. Schoukens, A. Hubin, P. Verboven, O. Blajiev, Electrochemical impedance spectroscopy in the presence of non-linear distortions and non-stationary behaviour: Part I: theory and validation, Electrochim. Acta. 49 (2004) 4753–4762. doi:10.1016/J.ELECTACTA.2004.05.039.

[51] O.L. Blajiev, R. Pintelon, A. Hubin, Detection and evaluation of measurement noise and stochastic non-linear distortions in electrochemical impedance measurements by a model based on a broadband periodic excitation, J. Electroanal. Chem. 576 (2005) 65–72. doi:10.1016/J.JELECHEM.2004.09.029.

[52] J.R. MacDonald, Impedance Spectroscopy – emphasizing solid materials and systems, Wiley, 1987.

[53] H. Nguyen Thi Le, B. Garcia, C. Deslouis, Q. Le Xuan, Corrosion protection and conducting polymers: polypyrrole films on iron, Electrochim. Acta. 46 (2001) 4259–4272. doi:10.1016/S0013-4686(01)00699-5.

[54] K. Cysewska, J. Karczewski, P. Jasiński, Influence of electropolymerization conditions on the morphological and electrical properties of PEDOT film, Electrochim. Acta. 176 (2015) 156–161. doi:10.1016/j.electacta.2015.07.006.

[55] G. Bereket, E. Hür, The corrosion protection of mild steel by single layered polypyrrole and multilayered polypyrrole/poly(5-amino-1-naphthol) coatings, Prog. Org. Coatings. 65 (2009) 116–124. doi:10.1016/J.PORGCOAT.2008.10.005.

[56] L.M. Duc, V.Q. Trung, Layers of inhibitor anion-doped polypyrrole for corrosion protection of mild steel, INTECH. 7 (2013) 143–174.